Seasonal decay of first-year sea ice: field measurements

Johnston, Michelle; Frederking, Robert

Publisher's version / Version de l'éditeur:
https://doi.org/10.4224/12340899
Technical Report (National Research Council of Canada. Canadian Hydraulics Centre); no. HYD-TR-057, 2000-09

CANADIAN HYDRAULICS CENTRE
CENTRE D'HYDRAULIQUE CANADIEN

SEASONAL DECAY OF FIRST-YEAR SEA ICE: FIELD MEASUREMENTS

M. Johnston and R. Frederking

Technical Report, HYD-TR-057

September 2000

National Research Council Canada
Conseil national de recherches Canada

CHC CANADIAN HYDRAULICS CENTRE

SEASONAL DECAY OF FIRST-YEAR SEA ICE: FIELD MEASUREMENTS

Interim Report
submitted to:

Robert L. Wolfe
Research and Development Officer
Transport Canada, Prairie and Northern Marine
Tower C, Place de Ville
14th Floor, 330 Sparks Street
Ottawa, Ontario K1A 0R6

and

Roger De Abreu
Environment Canada, Remote Sensing and Modelling
Canadian Ice Service
373 LaSalle Academy
Ottawa, Ontario K1A 0E6

Prepared By:

M. Johnston and R. Frederking
Canadian Hydraulics Centre
National Research Council of Canada
Montreal Road
Ottawa, Ontario K1A 0R6

Technical Report, HYD-TR-057

September 2000

ABSTRACT

This report describes the field program undertaken from 21 May to 19 July 2000 to measure the parameters that best characterize the ice decay process. During the field program, thickness of the first-year sea ice decreased from 1.55 m to 0.80 m, at which point the ice was virtually isothermal. The ice freeboard decreased from 60 mm in late May to a negative freeboard (melt ponding) in late July. Desalination was first observed in the surface layer of ice and eventually occurred in the bulk layer of ice, as indicated by the bulk salinity of 5 ‰ in late May and 0.5 ‰ in late July. More than one hundred borehole jack tests were conducted over the sampling period at depths 0.3, 0.6, 0.9 and 1.2 m. The average decrease in ice strength for the four depths was 8.7 MPa over the sampling period, most of which occurred between 4 June and 1 July. The surface layer of ice showed the largest decrease in strength over the sampling period (14.1 MPa to 2.1 MPa). Ice at a depth of 0.90 m had the least amount of change in strength (10.5 MPa to 3.7 MPa). In late July the bulk strength of the ice was only about 27% of what it was in late May.

TABLE OF CONTENTS

LIST OF FIGURES

LIST OF TABLES

SEASONAL DECAY OF FIRST-YEAR SEA ICE: FIELD MEASUREMENTS

1. INTRODUCTION

In Canada, the regulations presently in place to aid navigation in ice covered waters are being revised. Traditionally, the Zone/Date system has been used to regulate navigation in the Canadian Arctic based upon 16 zones. Individual zones were classified using historical data of the ice severity for a certain time of year. Since the Zone/Date System does not account for inter-annual differences in ice severity it has inherent limitations. Therefore a second system, one that relies upon up-to-date information about the ice conditions, was developed to augment the Zone/Date System. The new system is called the Arctic Ice Regime Shipping System (AIRSS) and it allows ships greater flexibility when navigating ice covered waters.

At present, AIRSS accounts for the deterioration of first-year sea ice only after the ice is in an advanced stage of melt, at which point it is considered *rotten*. Rotten ice has melt ponds over a significant portion of its surface and has ablated significantly. In reality, the ice decay process begins well before the ice has become rotten. At present, data on the properties of deteriorated ice during any stage of the decay process are extremely limited. This is because as soon as the ice begins to deteriorate it presents logistical difficulties for field measurement programs, which is why on-ice measurements typically have not extended beyond mid-May.

Canadian Hydraulics Centre designed the present a field program, whereby measurements of first-year sea ice would be conducted at various stages throughout the decay period. The requested field measurements were conducted by personnel from Canadian Ice Service, with field support from the University of Manitoba under the auspices of the Collaborative-Interdisciplinary Cryospheric Experiment (C-ICE'00). The measurement program was conducted over a nine-week period that extended from 21 May to 19 July 2000. During that time, the physical properties of the snow and ice were recorded, as were depth profiles of the ice strength. The acquired data were forwarded to Canadian Hydraulics Centre for analyses.

This report serves as an interim report, requested for incorporation into the C-ICE'00 field report, issued by the University of Manitoba. This report describes field techniques and measurements of decayed ice during the sampling period. The reader is referred to Johnston and Frederking (2000) for a complete description of the data analysis and the basis developed for incorporating first-year ice decay into the Arctic Ice Regime Shipping System (AIRSS).

2. BACKGROUND

Physical property measurements of first-year sea ice are generally conducted before mid-May, when the ice is still several degrees below freezing. Past studies have been conducted into the early melt season. Those studies focused upon properties of snow and the snow-ice interface. The snow-ice surface was emphasized because it is of primary importance to the remotely sensed imagery that is used for the daily ice charts issued by Canadian Ice Service (CIS).

During this study the surface properties and the bulk properties of the ice were measured over a nine-week period, from late May to late July. Property measurements that do not require direct physical contact with the ice are defined as *extrinsic* properties. Of relevance here are extrinsic properties that include air temperature, snow thickness and snow density (Table 1). The bulk physical properties of the ice, or so-called *intrinsic* properties, include the temperature, salinity and density of the full thickness of the ice and measurements of the ice borehole strength (*in situ* compressive strength).

Table 1 Factors Influencing Ice Decay

Measured Properties		Derived Parameters
Intrinsic Properties: Ice Surface	**Extrinsic Properties: Bulk Ice Cover**	
Air temperature Snow depth Snow density	Ice temperature Ice thickness Ice salinity Ice freeboard Ice borehole strength	Ice density Brine volume Total porosity Flexural strength Compressive strength

The intrinsic and extrinsic properties listed in Table 1 were used to calculate the ice density, brine volume and total porosity of the ice (sum of brine volume and air porosity). The total porosity was used to calculate the ice compressive strength (Timco and Frederking, 1990) and flexural strength (Timco and O'Brien, 1994) which were then correlated to the different stages of ice ablation, identified in Barber et al. (1997). This report presents a summary of the measurement techniques described in Frederking (2000) and provides a preliminary analysis of the data acquired during this field study. The reader is referred to Johnston and Frederking (2000) for complete details of the derived parameters listed in Table 1 and how they relate to the different stages of ablation.

3. FIELD MEASUREMENTS

The C-ICE'00 base camp was located on Truro Island in the Canadian Eastern Arctic Archipelago. The measurement site was located in an area of level first-year sea ice with a moderately thick snow cover and no signs of roughness or pressure ridging. Figure 1 shows the measurement site in late May. Ice of requisite character was located in McDougall Sound. The designated ice site was about 5 km east of base camp.

Figure 1 Measurement Site on First-year Ice in McDougal Sound (courtesy of K. Wilson)

The snow and ice properties were measured from 21 May to 19 July over a 900 m² area of ice. Each week, a field party visited the same area of ice by snowmobile and performed the requested measurements. Since visits were made twice per week during the latter stages of ice decay, data were acquired on a total of 11 days over the nine-week sampling period. Care was taken to ensure that the measurement stations (weekly or bi-weekly) were at least 5 m from each another.

3.1 Properties Measured at Each Hole

A motor driven, fibre glass corer was used to make a number of 150 mm diameter, smooth walled, vertical boreholes in the ice. Typically, a triangular pattern of three holes (plus or minus one borehole) was drilled in the ice. The holes were separated by a distance of about 1.5 to 2.0 m which minimized extraneous effects from ice damage caused by the coring process and the ice borehole strength tests.

The fibre glass corer provided a 100 mm diameter core. The ice cores from two of the holes were used to measure the bulk physical properties of the ice. The ice thickness, freeboard and snow depths at each hole were documented. A wooden straight edge was placed across the core hole to obtain a more precise measure of the ice freeboard, as shown in Figure 2.

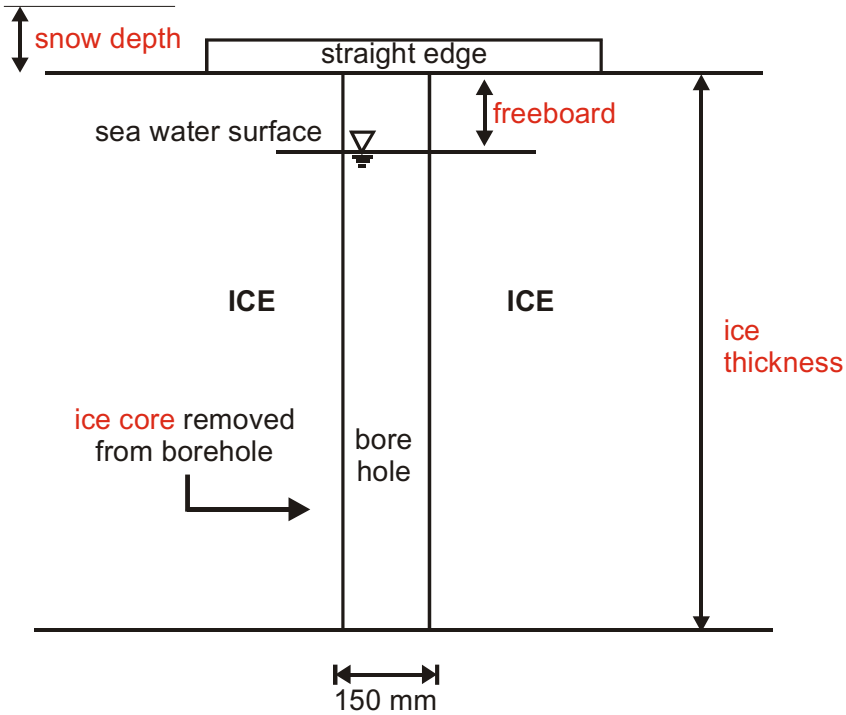

Figure 2 Measurements of Ice Thickness, Freeboard and Snow Depth

3.2 Borehole Jack Strength

The uniaxial compressive strength of the ice is fundamental to understanding ice induced loads on ships and offshore structures. Measurements of the uniaxial compressive strength require cutting beam specimens from the ice and applying a compressive stress along the longitudinal or lateral axis of the specimen. The borehole jack does not directly measure the uniaxial compressive strength of the ice, however, it can be used as an index of that parameter. Masterson et al. (1997) discuss the relationship between the ice borehole strength and the uniaxial compressive strength of the ice.

3.2.1 Borehole Jack Indentor System

The ice borehole strength (or *in situ* compressive strength) was measured at each of the three boreholes by lowering the borehole jack into the hole cut by the fibre glass corer (Figure 3). The borehole jack consists of a high-strength stainless steel hydraulic cylinder with a laterally acting piston. Once activated, the piston inside the body of the jack applies hydraulic pressure to the front and back indentor plates. The oil pressure is recorded digitally and can also be read from the dial gauge attached to the supply line.

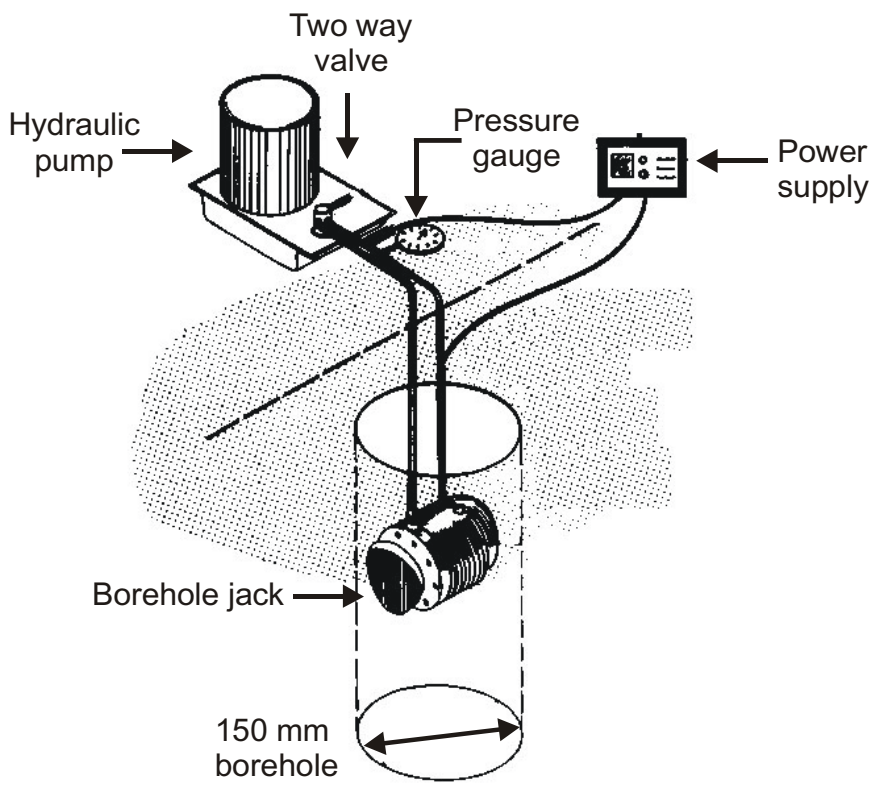

Figure 3 Borehole Jack Indentor Unit
(after Sandwell Inc., with adaptations)

The front and back indentor plates of the borehole jack are curved to match the wall of the borehole. Displacement of the indentor plates is measured using a linear, variable resistor mounted inside the jack body and attached to the front plate. The displacement is related to the resistance (measured at the surface with an ohmmeter) using a calibration curve. The penetration depth, or the depth that one of the indentor plates penetrates the ice, is calculated as one half of the total displacement of the two plates. The oil pressure and the total displacement of the indentor plates are recorded by an external digital acquisition system, details of which can be found in Frederking (2000).

3.2.2 Borehole Jack Tests

The borehole jack indentor was lowered into each borehole made by the fibre glass corer (Figure 4). Once positioned at the specified test depth, the borehole jack indentor plates were extended and the data were output to a digital data acquisition system. The indentor plates were extended continuously until the external pressure gauge showed a leveling off or decrease in the applied oil pressure. The plates were then retracted fully, the jack was rotated 90° and moved to the next test depth. Tests were conducted at a depth interval of 0.30 m until the bottom of the ice was reached at each hole. Measurements were made, typically, at four levels to an ice depth of 1.2 m.

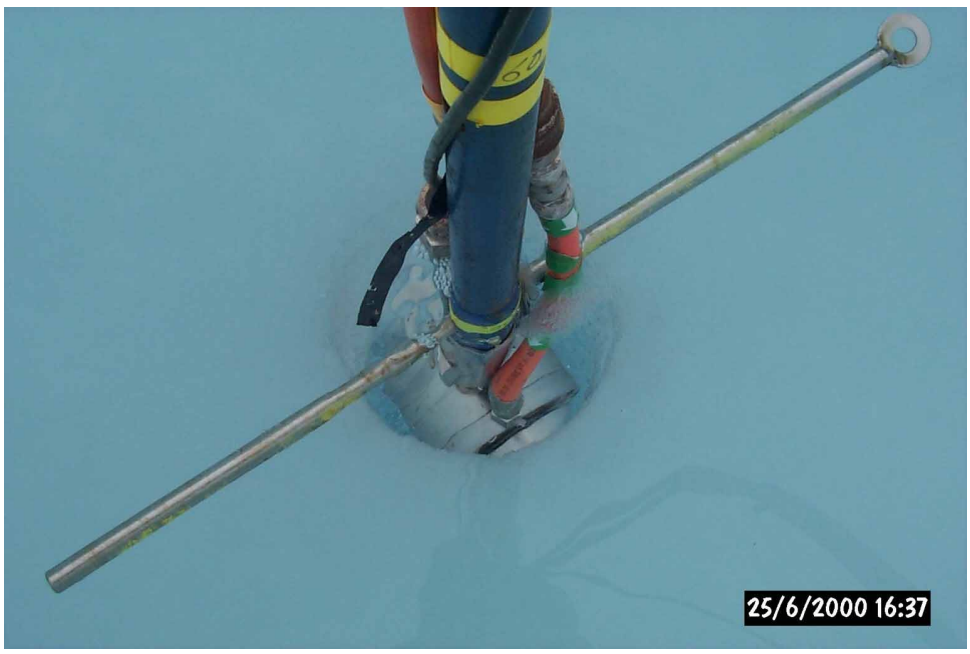

Figure 4 Borehole Jack Indentor
(courtesy of D. Bradley)

3.3 Ice Core Measurements

The full thickness core from the first hole was used for ice temperature measurements. A thermal probe was used to measure the ice temperature at 150 mm intervals. Due to a malfunction, the thermal probe did not provide instantaneous measurements of the ice temperature. The *in situ* ice temperature measurements from the nearby meteorological station were used in the subsequent data analysis.

The full thickness core from the second hole (Figure 5) was used to profile the ice salinity. Discs of ice, about 20 mm thick, were cut from the core at intervals of 150 mm. The ice discs were melted and used subsequently to measure the ice salinity with a calibrated conductivity meter. The core was sectioned as quickly as possible to minimize brine drainage. The core from the third hole was discarded, since it was not used for salinity or temperature measurements.

Figure 5 Typical Ice Core used for Salinity Measurements (1 July, courtesy of D. Bradley)

4. ACQUIRED DATA: PRELIMINARY ANALYSIS

This section summarizes the data acquired during the field program and describes changes in ice properties over the sampling period. The reader is referred to Johnston and Frederking (2000) for complete details of how the ice decay process is quantified using the properties measured during the field program.

4.1 Dates on which the Measurements were Performed

Ten visits to the main ice site were made between 21 May (Julian Day 142) and 19 July (JD201). By 18 July it was no longer safe to travel on the ice by snowmobile and the base camp on Truro Island was decommissioned. As a result, the site could not be accessed by snowmobile on 19 July. Rather, personnel from Canadian Ice Service (CIS) had the opportunity to use the Canadian Coast Guard vessel Louis S. St. Laurent (stationed in Resolute, Cornwallis Island) to make the final visit to the main ice site on 19 July.

The Louis S. St. Laurent enabled CIS personnel to access three additional ice sites between 19 and 20 July (Johnston and Frederking, 2000). On the afternoon of 19 July, the vessel stopped in central McDougall Sound to sample what was surprisingly thick first-year sea ice. The ice thickness at that site ranged from 1.5 m to over 2.1 m (limit of the ice auger). On 20 July two additional sites were sampled on the ice in Barrow Strait. The ice thickness at those sites ranged from 0.30 m to 1.15 m. The additional ice sites sampled in central McDougall Sound and Barrow Strait provide quantitative information about the most advanced stages of ice decay measured to date. Since there is no continuous record of the ice properties for those sites, however, those data can not be related directly to the nine weeks of decay measurements from the main ice site.

As the season progressed, certain areas of ice were covered by melt ponds, while other areas were characterized by slightly elevated, white, porous ice (Figure 6). The ice began to develop an undulating surface, indicating that the ice decay process was extremely non-uniform. Towards the end of the field program it became exceedingly difficult to locate level ice. As a result, measurements were taken in both ponded ice and hummocked ice. It is not known, presently, what effect that the different surface features had upon the measured strength of the ice. Since the following discussion is based upon an average of the properties measured at the individual boreholes at each station, it would not reflect those trends (if present).

Figure 6 Late Season Surface Topography of Decay First-year Sea Ice (21 July, courtesy of D. Bradley)

4.2 Air Temperatures throughout the Sampling Period

Figure 7 shows the daily mean air temperatures for Resolute Bay over the sampling period. The first measurements were acquired on 21 May (JD142) when the air temperature was –15°C. On JD162, the mean air temperature increased to +0.2°C, which was the first time that season that the mean air temperature rose above the melting point of sea ice (-1.8°C). The air temperature continued to increase as the season progressed and was punctuated periodically by near-freezing temperatures. The maximum air temperature recorded for the sampling period was +7.5°C on JD189 (7 July).

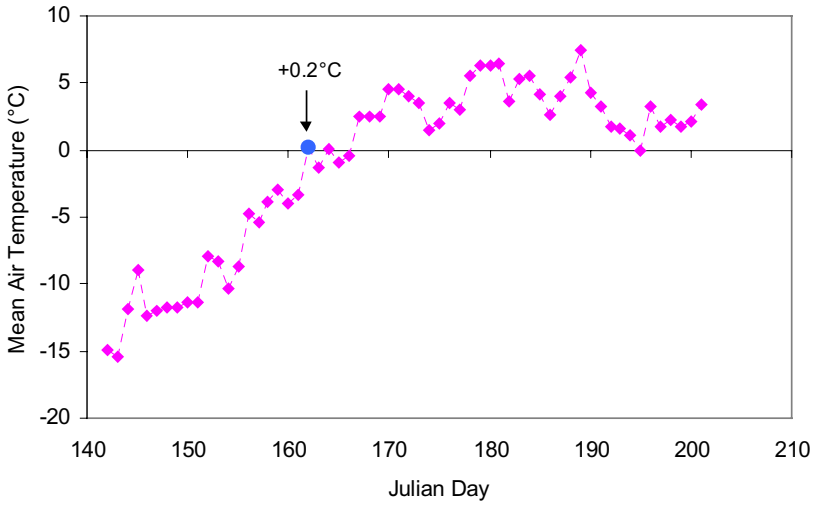

Figure 7 Mean Air Temperatures over the Sampling Period (data courtesy of the Atmospheric Environment Service)

4.3 Snow and Ice Thickness Measurements

Figure 8 shows the variation in the measured snow and ice properties over the sampling period. The data were obtained by averaging the measurements from all of the boreholes made at that station (two to four boreholes).

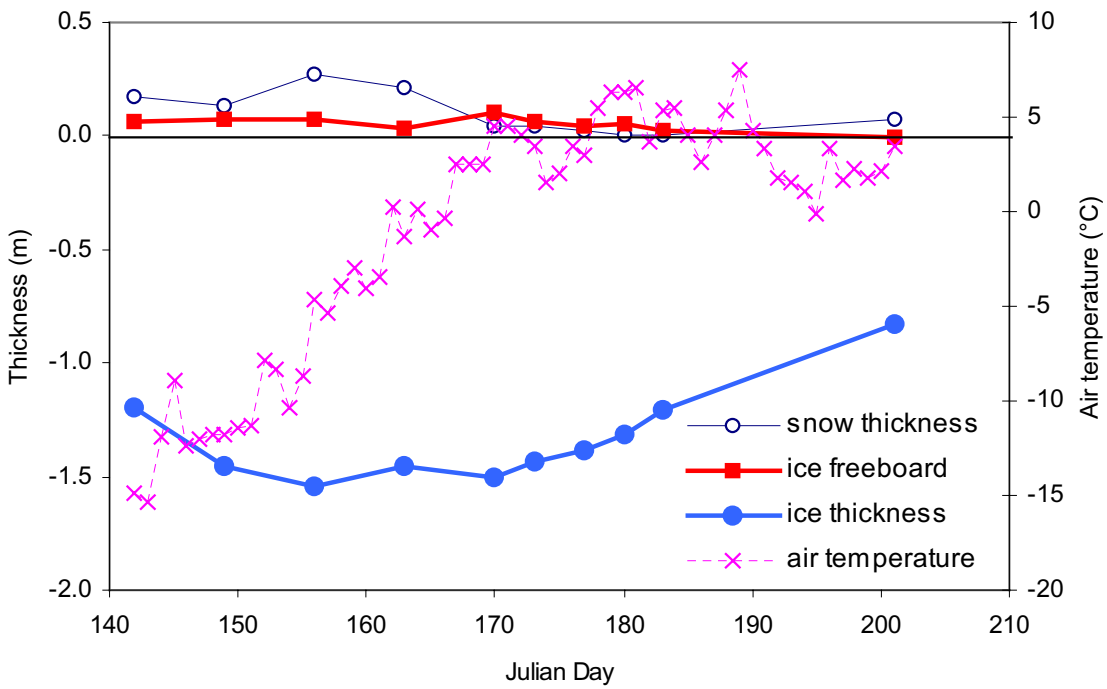

Figure 8 Variation in Measured Properties during the Sampling Period

When the measurement program commenced, the average snow cover thickness was 0.18 m and the ice was 1.47 m thick (Figure 8). Ice thickness measurements show that the continued cold temperatures resulted in ice growth until JD156, at which time the ice was 1.55 m thick. The increase in air temperature precipitated a rapid decrease in the snow cover thickness from 270 mm on JD156 to 40 mm on JD170. The warming air temperature and vanishing snow cover resulted in a decreasing trend in ice thickness that characterized the rest of the sampling period. The last recorded ice thickness at the main site was on JD201 (19 July) at which point the ice was 0.80 m thick.

4.4 Ice Freeboard

The continued ablation of the ice was accompanied by changes in the ice freeboard. Table 2 provides a better indication of the change in freeboard over the sampled decay period than Figure 8. Initially, the 1.47 m thick ice had a freeboard of 60 mm and an average ice temperature of –5°C (averaged over the full thickness, ice temperature is not reported in Figure 8). Around JD170 there was an increase in freeboard. In the advanced stages of decay the ice was nearly isothermal (above –1.8°C) and had lost nearly all of its freeboard.

The freeboard measurements on JD177 and JD201 need clarification, since two of the holes drilled at those stations were beneath melt ponds. A consequence of the averaging process is that the holes from the JD177 station appear to be covered by a melt pond (pond depth 13 mm, Table 2), yet have a measurable freeboard (43 mm). In fact, only one hole at the JD177 station was covered by a 40 mm deep melt pond. The other two holes from JD177 were on hummocked ice near the edge of the melt pond and had freeboards of 70 mm and 100 mm. Similarly, the negative freeboard reported for JD201 resulted from the averaging process (three of the four holes were in hummocked ice and the fourth hole was in a melt pond).

Table 2 Sampling Dates and Acquired Data

Date/ Julian Day	Ave. Snow depth (m)	Ave. Ice thickness (m)	Ave Freeboard (mm)	Ave. Pond depth (mm)	Bulk Salinity (‰)	Total number of BHJ tests
21 May/JD142	0.18	1.47	60	0	5.5	8
28 May/JD149	0.14	1.46	70	0	6.3	12
4 June/JD156	0.27	1.55	70	0	5.4	12
11 June/JD163	0.21	1.45	35	0	5.6	12
18 June/JD170	0.04	1.51	102	0	4.5	12
21 June/JD173	0.05	1.43	67	0	4.4	12
25 June/JD177	0.02	1.38	43*	13	4.0	12
28 June/JD180	0.01	1.31	50	0	3.6	12
1 July/JD183	0	1.21	20	0	--	7
19 July/JD201	0.08	0.82	11**	21	0.5	11

*average of –40, 100 and 70 mm, resulting in a negatively skewed freeboard/pond depth
**average of 55, 20, -85 and 55 mm, resulting in a negatively skewed freeboard/pond depth

4.5 Ice Salinity

An ice salinity profile for each of the weekly (and bi-weekly) stations was determined by sectioning one of the cores into 20 mm discs (at 150 mm intervals). Figure 9 shows the ice salinity profiles throughout the sampling period (salinity data for JD183 are not available). The warming trend that occurred from JD163 to JD170 (for air temperatures see Figure 7) caused the ice surface salinity to decrease from 11‰ to 1‰. During that time the salinity within the bulk layer of ice did not change substantially. By JD201, however, the salinity profile showed that the entire thickness of the cover had desalinated to less than 1‰.

Salinity measurements taken throughout the full thickness of one of the ice cores from each station were averaged to determine the bulk ice salinity (Table 2). In late May the ice had a bulk salinity of 5‰. By the end of the program (JD201/July 19) the bulk salinity had decreased to 0.5‰, as illustrated in Figure 9.

Elevated air (and ice) temperatures accelerated brine drainage from the cores while they were being extracted from the ice and as measurements were being taken. Although attempts were made to section the core as quickly as possible, brine drainage became increasingly problematic as the season advanced. As a result, the reported ice salinity profiles are less than would be representative of the *in situ* ice conditions.

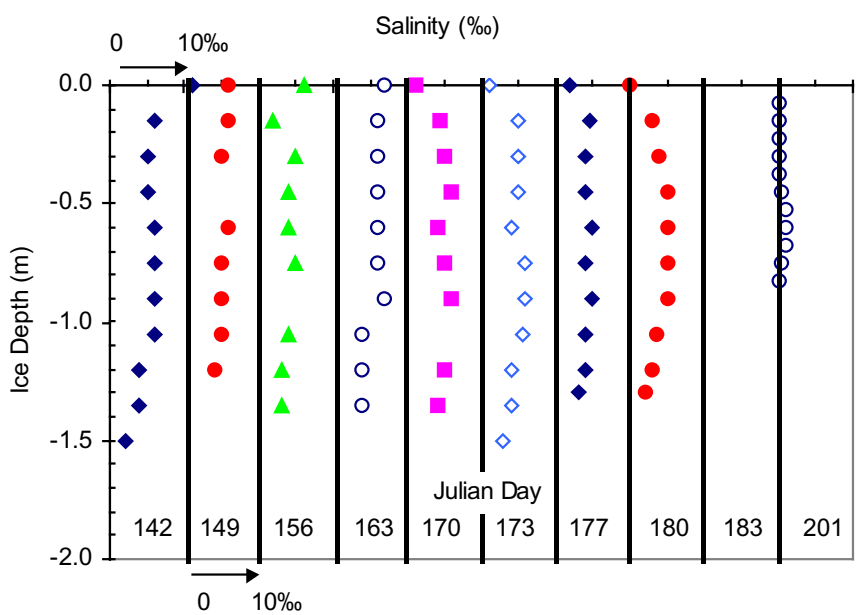

Figure 9 Salinity Profiles during Sampling Program (common scale of 0 to 10‰, with increments of 5‰)

4.6 Ice Borehole Strength

4.6.1 Representative Strength Data from Two Boreholes

Ten visits were made to the main ice site during the nine-week sampling period, resulting in a total of 110 borehole jack tests. Figure 10 shows the ice pressures measured in the **first borehole** (hole number 1) on JD142 (21 May) and JD201 (19 July). The pressures shown were measured at an ice depth of 0.30 m.

The disparity between the ice strength at the beginning and end of the sampling program (JD142 versus JD201) is the most notable feature of the load-time traces for the borehole shown in Figure 10. On JD142 (21 May) the surface layer at that hole had a maximum, measured borehole strength of 14.3 MPa. By late July the strength of the surface layer of ice in the first hole drilled on JD201 had decreased to 2.1 MPa.

There was a dramatic difference in the overall shape of the load-time traces from the beginning and end of the field program. On JD142, the pressure increased for the first 20 seconds, at which point the borehole jack was retracted and the ice pressure decreased. The pressure-time trace for JD201 was entirely different. In that case, the pressure reached a plateau after 6 seconds and remained at that level until the jack was retracted (after about 25 seconds).

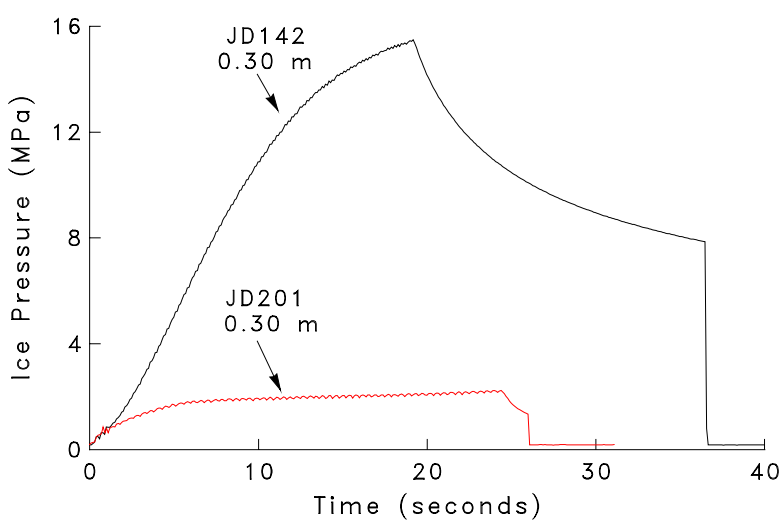

Figure 10 Ice Borehole Strength at the Beginning and End of the Sampling Period

Ideally, the borehole jack tests should be run over a period that is long enough to capture the leveling of pressure (as achieved in the test from JD201, shown above). Frequently, however, the series of ice borehole jack tests was not conducted long enough to capture a plateau in the ice pressure. This was due to limitations in the stroke of the ram (25 mm), concern about overloading the jack and the nature of a confined interaction test. Additionally, the maximum measured pressure was attained at different times for the each borehole jack test. As such, comparison of the different borehole jack tests required establishing a common factor. That factor was chosen as the ice pressure at the after one of the jack indentor plates had penetrated the ice 3 mm; a criterion that was universal in the borehole jack tests.

4.6.2 Variation in Strength Profiles with Time

The ice pressure-depth profiles were averaged over the number of boreholes at each station. Figure 11 shows the pressure depth profiles from late May (JD142) to late June (JD173). When the sampling period began on 21 May (JD142), the strength ranged from 10 to 14 MPa throughout the full thickness of the ice. The last borehole jack tests were conducted on 19 July (JD201), by which time the ice strength ranged from 2.1 MPa to 3.7 MPa. Examination of the 110 borehole jack tests conducted over the sampling period revealed that the bulk ice strength (averaged over the full thickness of the ice) was about 27% of the ice strength that was measured when the program began on 21 May (JD142).

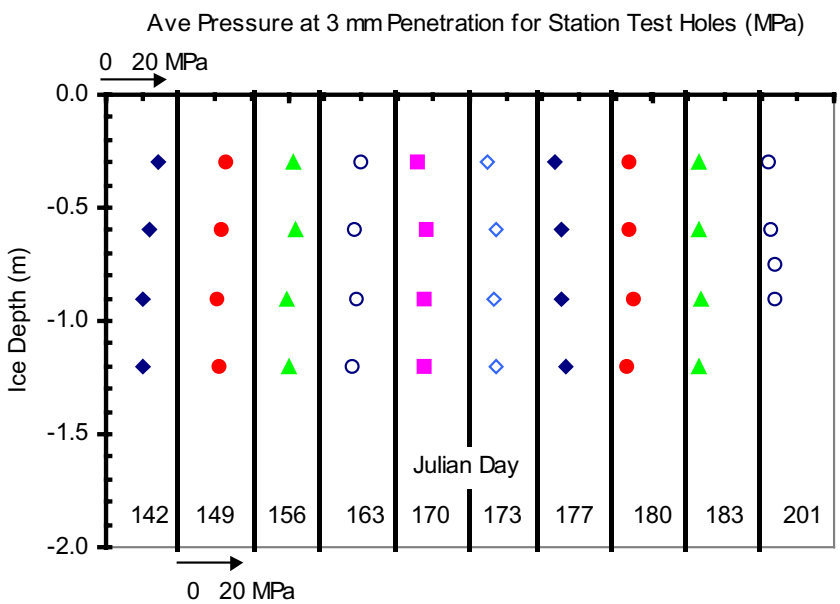

Figure 11 Depth Profiles of the Measured Ice Pressure at 3mm Penetration (common scale of 0 to 20 MPa with increments of 10 MPa)

4.6.3 Borehole Jack Data as function of Ice Depth and Time

Figure 12 shows the strength-time traces for the ice depths most commonly tested at the ice stations throughout the sampling period (0.3 m, 0.6 m, 0.9 m and 1.2 m). Changes in the ice borehole strength at 3 mm penetration are shown as a function of the Julian day on which the tests were conducted. Note that the reported strengths are the *average* borehole strengths (for a specific depth) of the holes tested at that particular station.

4.6.3.1 Ice Depth 0.3 m

The borehole jack tests (BHJ tests) at a depth of 0.30 m indicated that there was a gradual decrease in the ice strength during the first four weeks (JD142 to JD163, see Figure 12 a). The ice experienced a sharp decrease in strength (4.5 MPa) between the fourth and fifth weeks (JD163/June 11 and JD170/June 18). After the rapid drop in strength there was a gradual decrease in strength until the last tests were conducted on JD201 (19 July). Note that there was not much change in the ice strength during the last three weeks of the study (JD183 to JD201, change of 0.6 MPa). Since most of the change in ice strength occurred between the third and sixth weeks, the average rate of decay was calculated from JD156 to JD183 (from week 3 to week 6). The average rate of ice decay during that period was 0.45 MPa/day for ice at a depth of 0.30 m.

4.6.3.2 Ice Depth 0.6 m

While the ice at a depth of 0.30 m began to decrease in strength during the first three weeks of the program (JD142 to JD156), the ice strength at a depth of 0.60 m remained relatively unchanged (see Figure 12 b). The most significant change in strength at a depth of 0.60 m occurred between JD156 and JD163, when the ice strength decreased 4 MPa in 7 days. Ice at a depth of 0.60 m had an average rate of ice decay of 0.49 MPa/day between the third and sixth weeks (from JD156 to JD183).

4.6.3.3 Depth 0.9 m

The ice at a depth of 0.90 m showed the most uniform decline in strength during the first six weeks of the sampling period (JD142 to JD183). After JD183 (1 July, week 6), the ice strength appeared to plateau. By the end of the sampling period (JD201), the ice thickness at three of the drilled holes was 0.70 m, 0.80 m and 0.85 m. Since the fourth hole had an ice thickness of 0.95 m it the only data point used for JD201 in Figure 12 c. The average rate of ice decay between the third and sixth weeks (JD156 to JD183) was 0.31 MPa/day.

4.6.3.4 Depth 1.2 m

Figure 12 d shows that the bottom ice (depth of 1.2 m) experienced its most significant decrease in strength in late June (between JD 177 and JD180, week 6). Within three days, the ice strength decreased sharply by 3.0 MPa. The ice decay rate during the third and sixth weeks (JD156 and JD183) was 0.35 MPa/day.

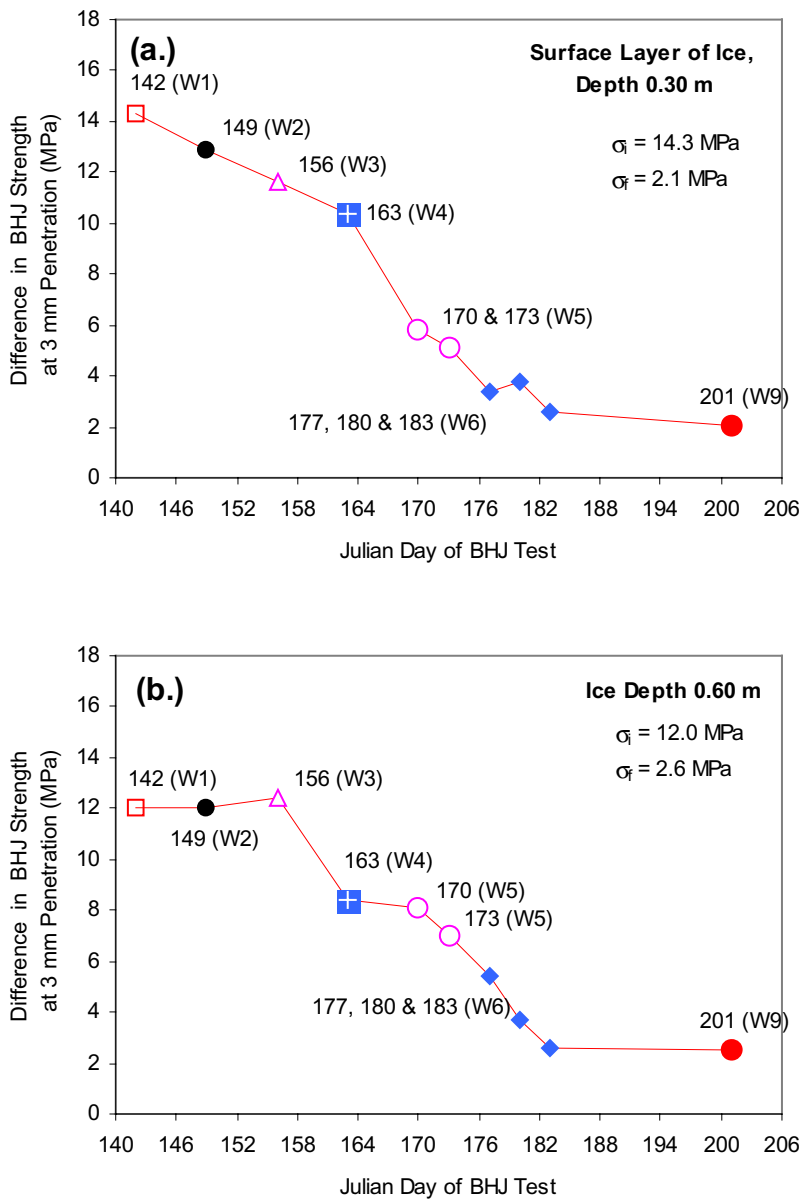

Figure 12 Ice Strength throughout the Sampling Period

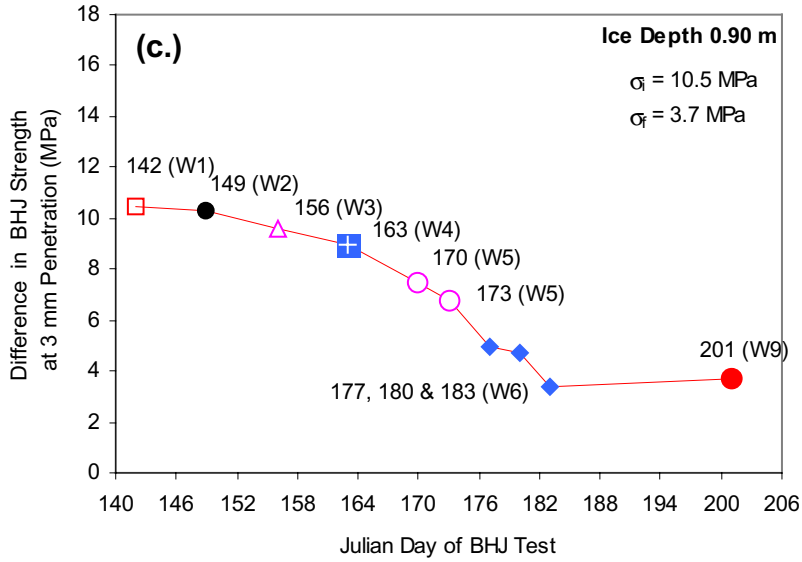

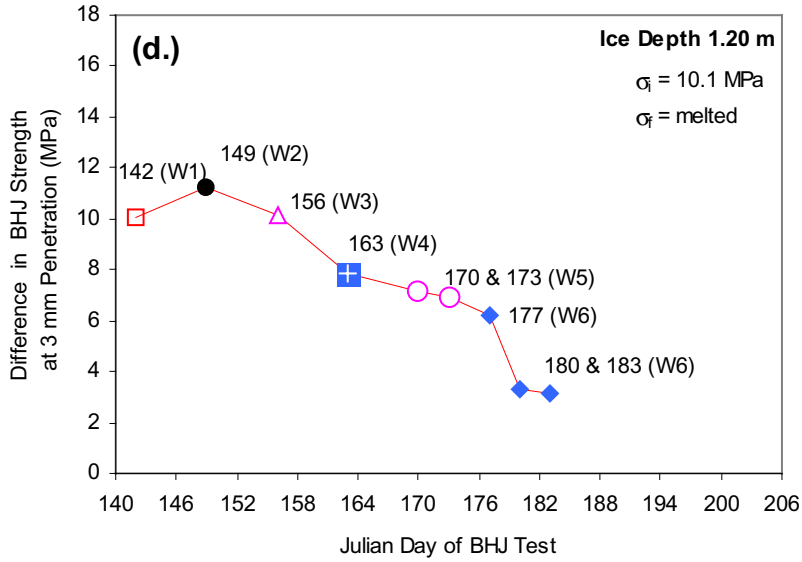

Figure 12 Ice Strength throughout the Sampling Period (continued)

5. CONCLUSIONS

This report described the field program undertaken from 21 May to 19 July to measure the parameters that best characterize the ice decay process. Measurements included temperature (air and ice), density (snow and ice freeboard), thickness (snow and ice), salinity and the ice borehole strength.

In situ ice temperatures recorded in late May showed a temperature gradient in the ice from –6°C at the ice surface to –1.8° at the ice-water interface. As the season progressed, the temperature gradient in the ice lessened. By the end of the study the ice had reached equilibrium around the melting point of sea ice (-1.8°C), indicating that the ice was virtually isothermal. As a result of the increased air temperatures, the snow pack rapidly melted and exposed the ice surface. Once exposed, the ice showed an enhanced rate of ablation. Between late May and late July, the thickness of the first-year sea ice at the main ice site decreased from 1.55 m to 0.80 m.

The reduction in ice thickness was accompanied by changes in the ice freeboard, which was an indirect indication of changes in the ice density and snow loading. The ice freeboard decreased from 60 mm in late May to a negative freeboard (melt ponding) in late July. The absence of freeboard in the later stages of the decay period indicated that the total porosity of the ice had increased substantially. The increased total porosity (brine pockets and air inclusions) resulted in the expansion and merging of what had been isolated pockets earlier in the season. Melt water and seawater infiltrated the pore spaces, causing the ice to become “water logged” and increasing the apparent density of the ice.

The ice salinity profiles measured throughout the season indicate that brine was continually being drained from the ice. Desalination was first observed in the surface layer of ice (the uppermost 0.30 m). As the ice continued to decay, it became less saline in the bulk layer of ice. The bulk salinity of the ice was 5‰ in late May and decreased to 0.5‰ by late July.

Determining the effect of morphological changes upon the strength of the ice required performing a series of borehole jack tests. Examination of the 110 borehole jack tests conducted over the sampling period revealed that most of the change in ice strength occurred in the three-week period between 4 June (JD156) and 1 July (JD183). During that time, the ice at the four tested levels decayed by 0.45, 0.49, 0.31 and 0.35 MPa/day (for ice at depths 0.3, 0.6, 0.9 and 1.2 m respectively). The surface layer of ice (depth 0.30 m) showed the largest decrease in strength over the sampling period (ice decay of 11.7 MPa between JD142 and JD201) yet did not have the highest *rate* of change. The ice at a depth of 0.60 m had the highest rate of change of 0.49 MPa/day (calculated

over the period JD156 to JD183). The ice strength at that depth, however, decreased a total of 9.4 MPa (versus the 11.7 MPa for the surface layer of ice). The bottom ice (depth 1.2 m) showed a strength decrease of 7.0 MPa over the sampling period. The least amount of change in strength occurred at a depth of 0.90 m, where the calculated decay rate was 0.31 MPa/day (from JD156 to JD183) and the total decrease in strength was 6.8 MPa over the sampling period. As a result, in late July the bulk strength of the ice (averaged over the full thickness of ice) was only about 27% of what it was in late May.

6. RECOMMENDATIONS

Having characterized the fundamental elements of the ice decay process, the field data may now be interpreted and used to determine how ice decay should best be incorporated into the Arctic Ice Regime Shipping Standards (AIRSS). Three of the necessary steps in achieving this objective are discussed in Johnston and Frederking (2000). The ice surface properties must be linked to the bulk ice cover properties, the measured properties must be related to the mechanical strength of the ice and a relation must be developed between the mechanical strength of the ice and the AIRSS Ice Numerals. There are two additional steps, beside the three just mentioned. Those tasks include developing a basis for adjusting the AIRSS Multipliers for ice decay and relating the modified Ice Multipliers to the Stages of Ablation. Only then may the information learned thus far be used successfully to adjust the AIRSS Ice Multipliers.

7. ACKNOWLEDGEMENTS

Transport Canada and Canadian Ice Service provided financial support for this project. Field measurements were undertaken by R. DeAbreu, K. Azmus, K. Wilson and D. Bradley of Canadian Ice Service. Field support from the University of Manitoba personnel is also gratefully acknowledged. Greatly appreciated is the support of Canadian Coast Guard in providing the Louis S. St. Laurent as a working platform from which to access first-year sea ice in its advanced stages of decay.

8. REFERENCES

Barber, D (1997) Sea Ice Decay: Phase I, Centre for Earth Observation Science, University of Manitoba, Winnipeg, Canada, March 1997, 108 pp.

Johnston, M. and R.M.W. Frederking (2000) Incorporation of Sea Ice Strength Decay into the Arctic Ice Regime Shipping System, report submitted to Transport Canada and Canadian Ice Service by Canadian Hydraulics Centre, HYD-TR-058 (in preparation).

Frederking, R.M.W. (2000) Testing the Compressive Strength of Sea Ice with a Borehole Jack: Field Instructions, report submitted to Canadian Ice Service by Canadian by Canadian Hydraulics Centre of the National Research Council of Canada, April 2000, Technical Report HYD-TR-055.

Borehole Jack Test Manual, report prepared by Sandwell Engineering Inc., Calgary Alberta, 31 March 2000, 13 pp.

Masterson, D.M, Graham, W.P., Jones, S.J. and G.R. Childs (1997) "A Comparison of Uniaxial and Borehole Jack Tests at Fort Providence Ice Crossing, 1995", Canadian Geotechnical Journal, Vol. 34, pp. 471 – 475.

Timco, G.W. and R.M.W. Frederking (1990) "Compressive Strength of Sea Ice Sheets", Cold Regions Science and Technology, Vol. 17, pp. 227 – 240.

Timco, G.W. and S. O'Brien (1994) "Flexural Strength Equation for Sea Ice", Cold Regions Science and Technology, Vol., 22, pp. 285 – 298.